

Morphological, thermal and mechanical properties of nanostructured materials based on polypropylene/poly (trimethylene terephthalate) blended fibers and organoclay

E. HEZAVEHI¹, A. BIGDELI², P. ZOLGHARNEIN^{1*}

¹ Textile Engineering Department, Faculty of Engineering, Islamic Azad University, Arak Branch, Arak, Iran

² Textile Engineering Department, Faculty of Engineering, Islamic Azad University, Science and Research Branch, Tehran, Iran

The crystallization morphologies, thermal behaviors and mechanical properties of PP/PTT/nanoclay blends nanocomposite fibers were investigated. Polypropylene/poly (trimethylene terephthalate) blends containing montmorillonite (MMT) were prepared using a twin screw extruder followed by fiber spinning process. The melt intercalation of PP and PPT alloys was carried out in the presence of a compatibilizer such as maleic anhydride-*g*-polypropylene (MAPP). The results show the improved adhesion between the phases and fine morphology of the dispersed phase. It has contributed to significant improvement in the properties and thermal stabilities of the final nanocomposite materials. A general understanding of how the morphology is likely to be related to the final properties of organically modified montmorillonite (OMMT)-incorporated PP/PTT blends is also described.

Keywords: *polypropylene, poly (trimethylene terephthalate), blend, organoclay, nanocomposite, morphology and properties*

© Wroclaw University of Technology.

1. Introduction

It is a common practice to make new polymer materials by blending or alloying of different polymers. However, it is difficult to obtain good dispersibility in polymer blends whose components are insoluble in each other, particularly for combinations of a non planar polymer with a polar one [1–3]. Therefore, the compatibilization is necessary for the immiscible polymer blends. It is usually achieved with block or graft copolymers, which exhibit intermolecular attraction or chemical reactions with the blend components. Maleic anhydride-*g*-polypropylene (MAPP) is an effective precursor of the reactive compatibilizers for PP and polar polymer blends [3].

The blending components of polyolefins and polyesters are important as they can improve the mechanical properties of the relatively weak constituents. The usage of polypropylene as one of the phases in polymer blends is widely preferred due

to its excellent processability and low cost. Several studies have been carried out on the blends of PP and PET to analyze their morphology and mechanical behavior [4–8]. The incorporation of PET fibers into PP to convert them into thermoplastic composites has been studied by Lopez and Arroyo [9]. In fact, the incorporation of PET fibers as a nucleating agent is of interest for the crystallization of PP [10, 11].

In the recent years, organic-inorganic nanocomposites have attracted great interest because of their high potential for applications as functional materials [12–15]. One of the most promising composite systems would be a hybrid based on organic polymers and layered silicates. The layered silicates are dispersed in the polymer matrix in the form of reticular layers of crystals about 1nm thick and with a lamellar aspect ratio of between 100 and 1000.

Because of the nanoscale structure, the nanocomposites possess unique properties not typically shared by conventional microcomposites [12]. A new approach in the nanocomposite studies involves nanocomposites based on blends of two or more

*E-mail: p.zolgharnein@gmail.com

polymeric materials [16–19]. In this field, some studies related to nanocomposites of the blends have been reported, especially for polypropylene/polyamide/6/clay (PP/PA6/clay) blends [19–22].

The incorporation of inorganic solid particles has been used as a method for stabilizing the blend morphology due to the compatibilization effect produced by the adsorption of the two polymers on the solid surface [23]. Moreover, the inorganic particles have also been used in toughening of polymers with the objective of introducing the enhancement of elastic properties in the blends apart from the improvement in toughness [24].

Recently, several research groups have shown that clay can effectively reduce the domain size of polymer blends and serve as compatibilizers in various immiscible polymer blends [25–29]. Most of them attribute this behavior to the ability of the clay to affect both the interfacial tension and the viscosity ratio, which are important factors in the determining of the dispersed phase size during mixing [30].

The organically modified nanoclay may act as a compatibilizer between the immiscible polymers. Yet the microscopy alone is not sufficient for concluding about the compatibilization role of the organoclay. Furthermore, as the short summary above indicates, there are three possible mechanisms of organoclay compatibilization (1) by the action of organic modifier (intercalant) miscible in both blend components, (2) by the solid- melt adsorption that results in free energy gains and (3) by migration to the interphase and modifying the interfacial tension between the two phases.

To get a better insight into the role of organoclay in polymeric blends, the immiscible polymers along with PP-g-MA were melt blended with modified montmorillonite MMT. Moreover, the amount of organoclay added to the various blends in the previous studies, was rather high, therefore an increase in viscosity could be the reason for the reduction in domain sizes [31–35]. This phenomenon was attributed to the fact that the two immiscible polymer chains can coexist between the intercalated clay platelets. These two chains play the role of a block copolymer, which acts as a compatilizer for the system [36].

The main objective of this work is to address the fundamental question of the role of compatibilization of the organoclay and maleic anhydride grafted polypropylene (PP-MA) in immiscible polymer blend nanocomposite fibers.

2. Experimental

2.1. Materials

Commercial grade of isotactic PP fiber, known as V30S, was supplied from Arak Petrochemical Co., Iran. The flow index (MFI) of the PP melt was 16 g/10 min, its density amounted to 0.92 g/cm³ and T_m was 166 °C. The fiber grade PTT was produced by Shell Chemical Co with trade name of CORTERRA 9240. PP-g-MA (trade name PB3150) was received from Uniroyal Chemical Co., USA. This polypropylene has the MFI of 50 g/10 min, MAH index of 1.5% and density of 0.9 g/cm³. The organically modified montmorillonite nanoclay (Cloisite15A) supplied by Southern Clay Products Inc., was used as received for the melt blending.

2.2. Specimen preparation

PTT, MAPP and nanoclay were dried in a vacuum oven for 24 h at 80 °C. To obtain the sufficient amount of material for mechanical property test, melt compounding was also conducted by using a co-rotating twin screw extruder (Z-sky). The temperatures in the extrusion zone ranged from 220 to 240 °C and the screw speed of 120 rpm was adjusted (the mixing time was less than 3 minutes).

The extrudates were palletized with Haake pelletizer. The blend compositions are given in Table 1. Before the melt spinning, the polymer blends were dried in a vacuum oven for 24 h at 80 °C. The melt spinning process was performed with a single screw (L/D = 26) Brabender melt extruder with a spinneret containing 20 orifices, each of 0.5 mm in diameter. The extruder was set with five different temperature zones, 200, 210, 230, 240 and 250 °C, respectively, at the feeding, metering, die and spinneret section. The screw was run at 60 rpm.

Table 1. Blending compositions.

Sample	PP%	%PTT	%MAPP	%Nano Clay
1	80	15	5	–
2	70	25	5	–
3	60	35	–	–
4	75	25	5	–
5	79	15	5	1
6	77	15	5	3
7	75	15	5	5

3. Characterization

3.1. Scanning electron microscopy (SEM)

SEM images were taken to study the morphology of PP/PTT blends with and without nanoclay and compatibilizer. SEM micrographs were taken from cryogenically fractured surface of polyblend samples after submersion in liquid nitrogen for 1 h. The surface was then sputter coated with gold palladium before viewing. The fractured surfaces of the samples were investigated with a SEM, LE0440, operating at 20 kV.

3.2. Thermal analysis (DSC and TGA)

Differential scanning calorimetry spectra were recorded with Perkin-Elmer DSC pyres-I. The temperature of the calorimeter was calibrated with indium, and then the crystallization process was carried out. All DSCs experiments were performed under nitrogen atmosphere. In this experiment, about five milligrams of dried sample was first kept at 50 °C for 0.5 min, then heated quickly from 50 to 350 °C at 30 °C/min and kept for 5 minutes after reaching 200 °C in order to eliminate the influence of thermal history. Afterwards, the samples were cooled from 350 to 50 °C (at 10 °C/min) and kept at 50 °C for 1 minute. Finally, a heating scanning from 50 to 350 °C (at 5 °C/min) was carried out. The thermogravimetric experiment was performed with a Perkin-Elmer TGA7 thermal analysis system. The TGA scans were recorded at 10 °C/min under a nitrogen atmosphere from 50 to 700 °C.

3.3. X-ray diffraction analysis (XRD)

A Siemens X-ray diffraction unit operated at 30 kV and 20 mA, with Cu element and nickel filter

was used to observe the changes in the crystallinity of samples.

3.4. Mechanical test

The mechanical properties of the fibers were measured using an Instron tensile testing machine. The data were collected by a computer. The tensile modulus was measured as the slope of the stress-strain curve using a 10 % min⁻¹ strain rate and a 500 g load cell. No slippage of filaments in the grips was detected during the testing by this method. The average mechanical properties of ten filaments were tested for each composition.

4. Results and discussion

4.1. Morphology of PTT domain

A comparative study of the phase morphologies of the blends was performed with SEM. PP and PTT are immiscible polymers, and the PTT appeared as a disperse phase with irregular shape in the PP matrix (Fig. 1). The samples were analyzed at perpendicular direction to the spinning flow (transverse direction) and parallel to the spinning flow (longitudinal direction). The strain below the spinneret could deform the PTT phase in the fiber path.

The white domains in the SEM images represent the position of the PTT dispersed phase in the PP matrix (Fig. 1). Both the interparticle distance and the size of the dispersed PTT phase are found to decrease on adding the nanoclay. However, due to the complexity of flow in the extruder, it is difficult to assert that the nature of the flow is responsible for the obtained morphology. Regarding the coalescence mechanism, nanoclay layers lower the coalescence rate and, consequently, promote the droplet size reduction as the balance between breakup and coalescence is shifted to the breakup mechanism. This could be explained by the fact that the polymer pairs of PP and PTT are thermodynamically immiscible. To play this role, nanoclay should be at least partially exfoliated and should interact with both phases.

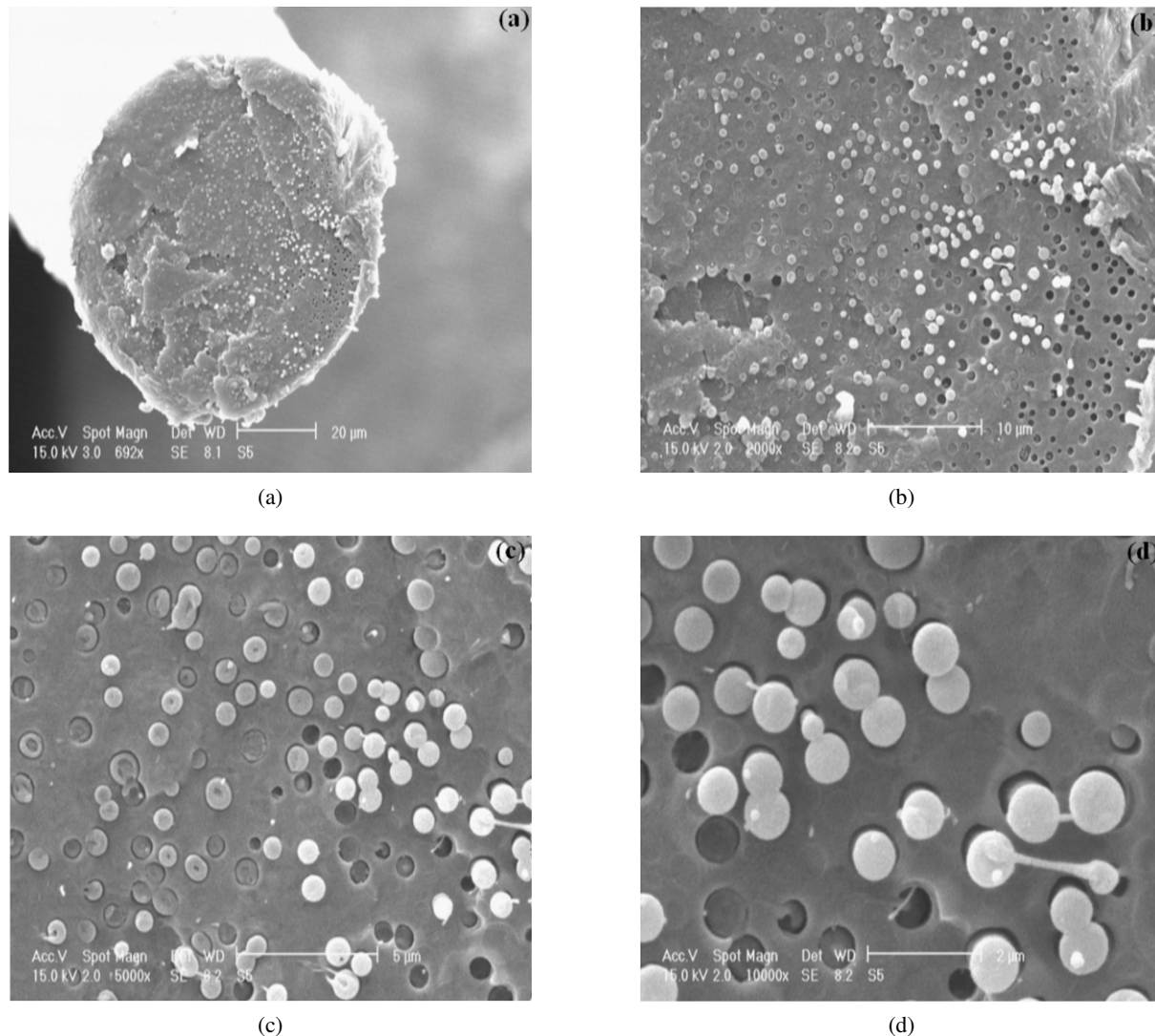


Fig. 1. SEM micrographs of the 1% nanoclay filled PP/PTT/MAPP (79/15/5 by wt%) blend nanocomposite fibers at four different magnifications with different optical resolution; a) 692 \times ; b) 2000 \times ; c) 5000 \times ; d) 10000 \times .

4.2. Thermal analysis

The results of DSC analysis of the samples are summarized in Table 2. As can be seen from the DSC results, the polyblend fibers and nanocomposite fibers exhibit two distinct melting peaks, the lower obviously corresponding to the melting point of PP, whereas the higher corresponding to the melting of PTT. Since the neat PP and PTT fibers show only one melting peak, each of two polymers could be in general considered as immiscible.

The melting temperature of PP does not appear to be different in most polyblends and polyblend

nanocomposite fibers in comparison to that of the neat PP fiber. The T_m of PTT in polyblend and polyblend nanocomposite fibers, on the other hand, was consistently by 2 $^{\circ}\text{C}$ lower than the value of the corresponding neat fiber.

Probably, the lower T_m of PTT in the fibers can be a result of the formation of a block copolymer between PP-g-MAH and PTT. One of the observed results is that the crystallinity of PTT in the polyblend fibers is higher than the value of the neat fibers.

Most probably, this indicates that PP moieties act as nucleating agents for PTT in the polyblend

Table 2. DSC thermal properties and the percentage of crystallinity for the fibers.

Samples	T _m of PP (°C)	T _m of PTT (°C)	Crystallinity PP (%)	Crystallinity PTT (%)	Total Crystallinity (%)
PP	166.5	–	37.03	–	37.03
PTT	–	231.3	–	23	23
2	167.7	229.2	42.2	33.92	40.1
3	167	229.3	39.62	19.7	38.2
4	167.9	229.4	50	25.58	41.5
5	166.7	228.5	47	23	40.6
7	167.3	228.8	47.15	19.9	38.25

fibers. A similar increase in crystallinity does not occur in PP. Such nucleating effect was often reported for organoclays and compatibilizers. The crystallization of the PTT phase increased slightly with the addition of organoclay, and the increment was a bit more distinct for MAH-g-PP compatibilized PP/PTT polyblend nanocomposite fibers.

The TGA curves were taken from the organoclay after being exposed to a temperature of 600 °C, which resulted in 70 wt% ashes content. Therefore, the total weight loss of 30 % could be attributed to the decomposition of octadecylamine that intercalated in the montmorillonite galleries. The remaining ashes can be attributed to the high thermal stability of montmorillonite. This result was in concord with the data sheets of the organoclay supplier. It is generally accepted that the incorporation of layered silicate platelets into polymeric materials can improve their thermal stabilities.

In case of clay-containing polymer nanocomposites, the increase in thermal stability can be attributed to an ablative reassembling of the silicate layer which may occur on the surface of the nanocomposites creating a physical protective barrier on the material.

On the other hand, volatilization might also be delayed by the labyrinth effect of the silicate layer dispersed in the nanocomposites. However, the improvement in thermal stability of polymer/clay nanocomposites is directly related to the degree of dispersion of silicate layers in the polymer matrix. In the case of polymer blend nanocomposites, the thermal stability is also controlled by the final morphology of dispersed phase. Figs. 2a to 2g show the typical TGA traces of weight loss as a function

of the measured temperature and pyrolytic environments.

4.3. Wide angle X-ray diffraction analysis

The 2θ X-ray diffraction patterns of polyblend and polyblend nanocomposite fibers are shown in Figs. 3a to 3g. There are no significant shifts in the diffraction positions of the two materials after forming the polyblend and polyblend nanocomposite fibers. This shows that the nature of the crystalline lattices of the two materials did not undergo an appreciable change. The intensity of the reflections at the angular positions 2θ of 14.2, 116.8 and 18.6 corresponding, respectively to the (110), (040), and (130) planes of PP and 2θ of 15 corresponding to the (010) plane of PTT actually increased. This suggests that each polymer component has a tendency to enhance the size and/or perfection of the crystals in the polyblend fibers.

4.4. Mechanical properties

Tensile strength, modulus, and elongation at break of different PP/PTT blend fibers with and without nanoclay and compatibilizer are listed in Fig. 4. The test results showed that the addition of PP-g-MA indeed improves the compatibilization of the PP/PTT blends, which seem to be better than pure PP fibers because of the formation of in situ micro-PTT fibrils. The PP/PTT/MAPP/Nanoclay blended nanocomposite fibers have better mechanical properties than the blend.

It was found that the presence of a compatibilizer plays a significant role in determining the organoclay partitioning and the extent of improvement

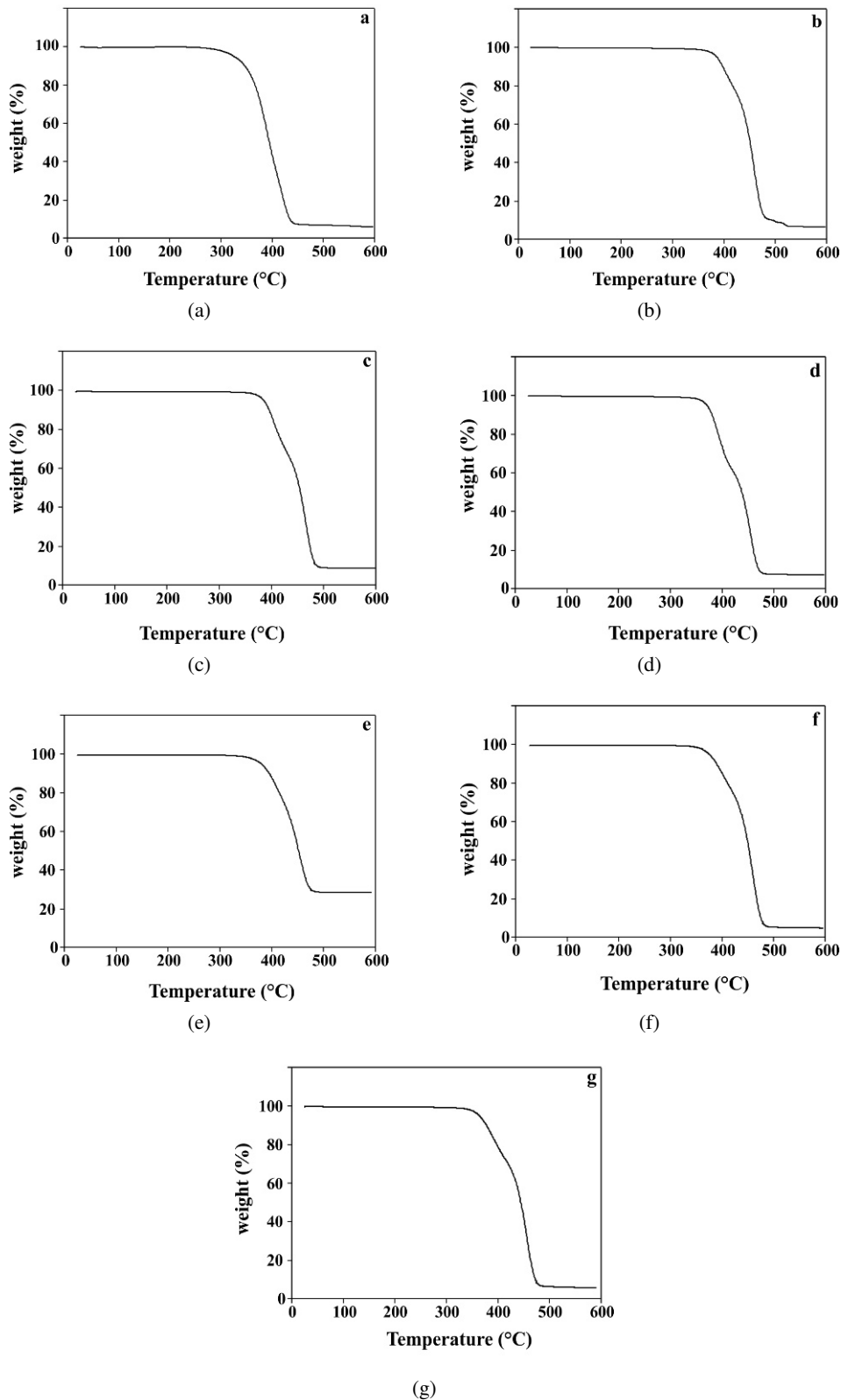


Fig. 2. TGA diagrams of polyblend and polyblend nanocomposite fibers: a) sample 1; b) sample 2; c) sample 3; d) sample 4; e) sample 5; f) sample 6; g) sample 7.

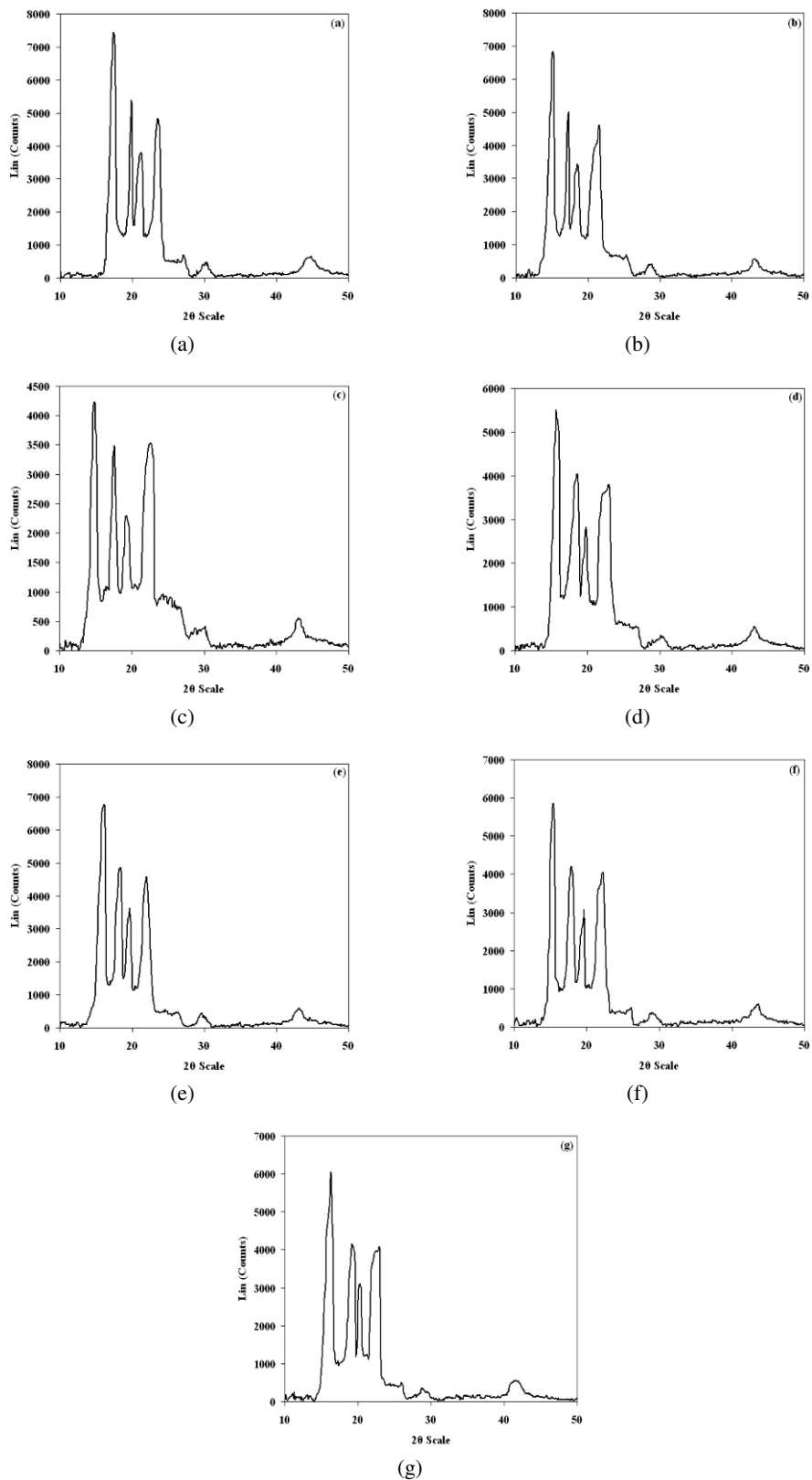


Fig. 3. Wide angle x-ray diffraction spectra: a) sample 1; b) sample 2; c) sample 3; d) sample 4; e) sample 5; f) sample 6; g) sample 7.

of its mechanical properties. This improvement in tensile strength and tensile modulus of the polyblend fibers containing nanoclay is thought to depend on the interactions between the polar polymer molecules and the layered organoclay, as well as on the rigidity of the clay layers themselves.

Indeed, the rigidity of the clay layers is considerably greater than the polymer molecules and thus they do not deform or relax to the same extent.

4.5. Proposed morphology

Fig. 5 shows a schematic representation of the morphology of the MAH-g-PP compatibilized PP/PTT nanocomposites containing organoclay. This scheme is proposed based on the collective results obtained with SEM, DSC, XRD, and mechanical properties. The proposed morphology shows partially exfoliated silicate layers distributed in both phases. However, there are also some layered silicate agglomerates which coexist with the exfoliated and intercalated ones in the PTT phase. The mean particle size of PTT (droplets) is smaller in the presence of the MAH-g-PP compatibilizer than in its absence. Thus, the MAH-g-PP acts as an effective compatibilizer by forming PTT-g-PP copolymer, as indicated in the scheme. The scheme in Fig. 5 also indicates the interaction between the amine groups of the octadecylamine intercalate of the exfoliated organoclay and ester groups of the PTT and PTT-g-PP copolymer.

In fact, the compatibilizer can stay in both matrix and dispersed phase during melt mixing, hence, the real viscosity ratio must be between these two phases. In other words, it would ascend with increasing the compatibilizer content. PP-g-MA has the group which reacts with PTT chains during melt blending and the reaction scheme is shown in Fig. 6.

5. Conclusions

In this study, the effect of addition of organically modified nanoclay and PP-g-MA at different blend ratios on the morphology and properties of immiscible polypropylene/poly (trimethylene terephthalate) blend fibers was investigated. The compatibility of PP/PTT blends can be considerably improved by the addition of nanoclay and PP-g-MA, which have an

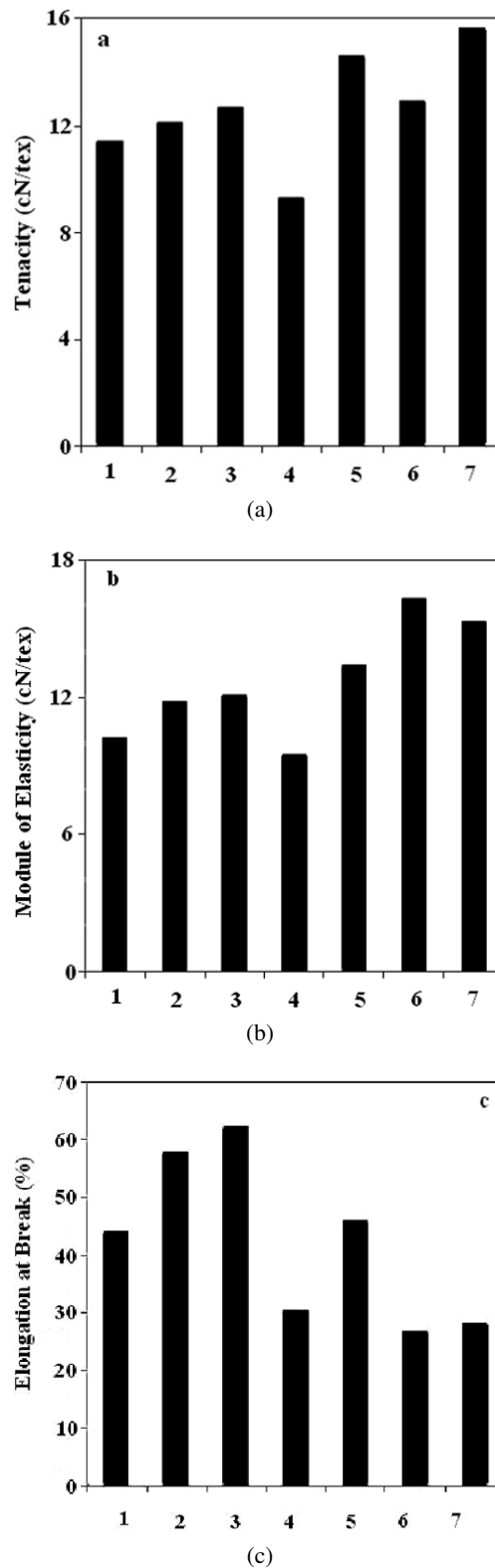


Fig. 4. Tensile properties of hybrid fibers: a) tenacity (cN/tex), b) module of elasticity (cN/tex), c) elongation at break (%).

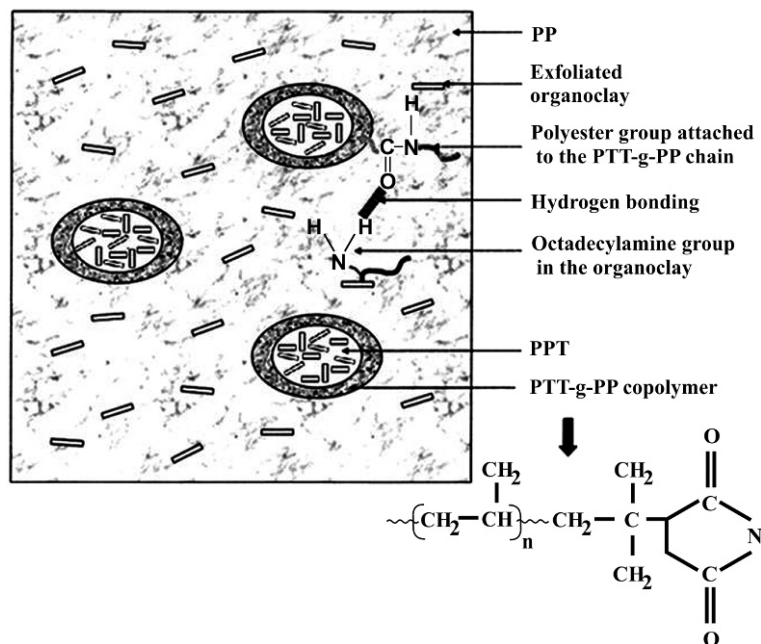


Fig. 5. Sketch the morphology of MAH-g-PP compatibilized PP/PTT/organoclay polyblend nanocomposite fibers.

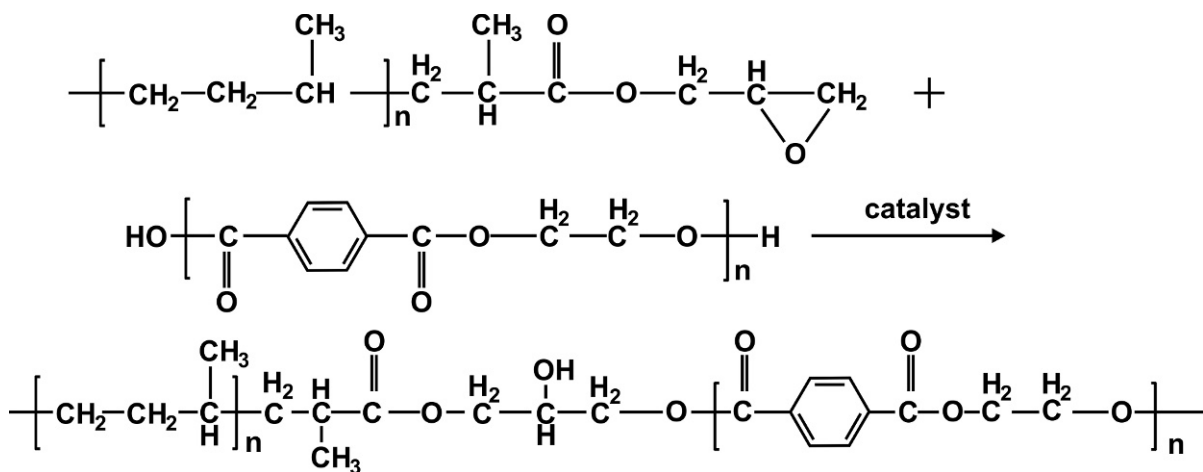


Fig. 6. Reaction scheme between PP-g-MA and PTT.

excellent effect on reducing the interfacial tension. Selective localization of nanoclay at the interface of immiscible PP/PTT polymer blend can be achieved by introducing a copolymer that preferentially localizes at the blend interface and has the highest affinity to the nanoclay.

PTT disperse phase, similar to nanoclay in serving as a heterogeneous nucleation agent, could en-

hance the crystallization of PP. The tensile strength and Young's modulus of the blend and blend nanocomposite fibers were improved due to the strong interface bonds between the matrix and the dispersed phase. The PTT domains were less susceptible to deformation in the PP/PTT/MAPP/nanoclay blend during the process than in the PP/PTT/MAPP. The optimum result was observed when PP-g-MA

and nanoclay were used simultaneously. The crystallization, melting behavior and polymorphic composition of PP in non-compatibilized and the compatibilized PP/PTT blends are related to PTT content, compatibilizer and nanoclay content. The proposed model has shown that the behavior of complicated multi-component nanoclay containing polymer blend system can be explained with the aid of a number of simplified model systems.

References

- [1] WILKINSON A.N., LAUGEL L., CLEMENS M.L., HARDING V.M., MARIN M., *Polymer*, 40 (1999), 4971..
- [2] ROEDER J.O., LIVEIRA R.V.B., GONCALVES M.C., SOLDI V., PIRES A.T.N., *Polymer test*, 21 (2002), 815..
- [3] TSENG F.P., LIN J.-J., TSENG C.R., CHANG F.-C., *Polymer*, 42 (2001), 713.
- [4] PAPADOPOULOU C.P., KALFOGLOU N.K., *Polymer*, 41 (2004), 2543.
- [5] LEPERS J.C., FAVIS B.E., TABAR R.J., *Polymer Sci. Polymer Phys.*, 35 (1997), 2271.
- [6] PANG Y.X.D., JIA M., HU H.J., HOURSTAON D.J., SONG M., *Polymer*, 41 (2000), 351.
- [7] BAE T.Y., PARK K.Y., KIM D.H., SUH K.D., *Appl. Polymer Sci.*, 81(5) (2001), 1056–1062.
- [8] SONG M., PANG Y.X., *Macromol. Sci. Phys. b*, 40 (2001), 1151.
- [9] LOPEZ M.Z., ARROYO M., *Polymer*, 41 (2000), 7761.
- [10] WANG C., LIU CR., *Polymer*, 38 (1997), 4715.
- [11] SAUJANYA C., RADHAKRISHNAN S., *Polymer*, 42 (2001), 4537.
- [12] ALEXANDER M., DUBOIS P., *Master Sci. Eng.*, 18(1–2) (2000), 1.
- [13] YONG T., YUAN H., SHAO F.W., ZHOU G., ZU Y., WEI CF., *Polym. Degrad. Stab.*, 78(2002) 555.
- [14] HU Y., SONG L., JXU L., CHEN Z., FAN W., *Colloid Polymer Sci.*, 279 (2001), 819.
- [15] GILMAN J., *Appl. Clay Sci.*, 15 (1999), 31.
- [16] ZARAGOZA M., VARGAS E.R., RODRIGUEZ F., MARTINEZ B.M.H., *Polymer Degrad. Stab.*, 91 (2006), 1319.
- [17] LI C., XIAO Y., GUAN G., LIU X., ZHANG D., *Appl. Polymer Sci.*, 101 (2006), 2512.
- [18] FROUNCHI M., DADBIN S., SALEHPOUR Z., NOFERESTI M., *Membr. Sci.*, 282(1–2) (2006), 142.
- [19] ZOU H., ZHANG Q., TAN H., WANG K., DU R., FU Q., *Polymer*, 47 (2006), 6.
- [20] CHOW W.S., BAKER A.A., ISHAK Z.A.M., KARGER-KOCSIS J., ISHIAKU US., *Eur. Polymer. J.*, 41 (2005), 687.
- [21] GAHLEITNER M., KRETZSCHMAR B., VAN VLIET G., DERAUX J., POSPIECH D., BERNREITNER K., INGOLIC E., *Rheol. Acta*, 45(4) (2006), 322.
- [22] GAHLEITNER M., KRETZSCHMAR B., POSPIECH D., INGOLIC E., REICHELT N., BERNREITNER K., *Appl. Polymer Sci.*, 100(1) (2006), 283.
- [23] TANG Y., HUA Y., ZHANG R., GUI Z., WANG Z., CHEN Z., FAN W., *Polymer*, 45 (2004), 5317.
- [24] LIPATOW YS., *Polymer Sci.*, 27 (2002), 1721.
- [25] ARGON A., COHEN R.E., *Polymer*, 44(19) (2003), 6013.
- [26] HONG J.S., NAMKUNG H., AHN KH., LEE S.J., KIM C., *Polymer*, 47(11) (2006), 3967.
- [27] KHATUA B.B., LEE D.J., KIM H.Y., KIM J.K., *Macromolecules*, 37(7) (2004), 2454.
- [28] SI M., ARAKI T., ADE H., KILCOYNE A.L.D., FISHER R., SOKOLOV J.C., RFAILOVICH MH., *Macromolecules*, 39(14) (2006), 4793.
- [29] HONG J., KIM Y.K., AHN K.H., LEE S.J., KIM C., *Rheol. Acta*, 46 (2007), 469.
- [30] RAY S.S., POULIOT S., BOUSIMINA M., UTRACKI L.A., *Polymer*, 45(25) (2004), 8403.
- [31] HASEGAWA N., OKAMOTO H., KATO M., USUKI A., *Appl. Polymer Sci.*, 78(11) (2000), 1918.
- [32] GALGALI G., RAMESH C., LELE A., *Macromolecules*, 34(4) (2001), 852.
- [33] WANG S., HU Y., SONG L., LIU J., CHEN Z., FAN WJ., *Appl. Polymer Sci.*, 91(3) (2004), 1457.
- [34] SINHA RAY S., OKAMOTO M., *Polymer Sci.*, 28 (2003), 1539.
- [35] XING P., BOUSMINA M., RODRIGUNE D., KAMAL MR., *Macromolecules*, 33(21) (2000), 8020.
- [36] WANG Y., ZANG Q., FU Q., *Macromol Rapid Commun.*, 24(3) (2003), 231.

Received 28.06.2011

Accepted 31.05.2012